# ANALYSIS OF ELECTRIC CURRENT HELICITY IN ACTIVE REGIONS ON THE BASIS OF VECTOR MAGNETOGRAMS

V. I. Abramenko

*Crimean Astrophysical Observatory, 334413, Nauchny, Crimea, Ukraine; and Beijing Astronomical Observatory, Chinese Academy of Sciences, Beijing 100080, China*

Tongjiang Wang

*Beijing Astronomical Observatory, Chinese Academy of Sciences, Beijing 100080, China*

V. B. Yurchishin

*Crimean Astrophysical Observatory, 334413, Nauchny, Crimea, Ukraine; and Beijing Astronomical Observatory, Chinese Academy of Sciences, Beijing 100080, China*

**Abstract**. The problem of (dc) magnetic field energy build up in the solar atmosphere is addressed. Although large-scale current generation may be due to large-scale shearing motions in the photosphere, recently a new approach was proposed: under the assumption that the magnetic field evolves through a sequence of force-free states, Seehafer (1994) found that the energy of small-scale fluctuations may be transferred into energy of large-scale currents in an AR (the alpha-effect). The necessary condition for the alpha-effect is revealed by the presence of a predominant sign of current helicity over the volume under consideration. We studied how frequently such a condition may occur in ARs.

On the basis of vector magnetic field measurements we calculated the current helicity $B_z \cdot (\nabla \times \mathbf{B})_z$ on the photosphere over the whole AR area for 40 active regions and obtained the following results:

1) In 90% of cases there existed significant excess current helicity of some sign over the active region area. So one can suggest that the build up of large-scale currents in an active region due to small-scale fluctuations may be typical in ARs.

2) In 82.5% of cases the excess current helicity in the northern (southern) hemisphere was negative (positive).

The method proposed can be applied to those ARs where the determination of the predominant sign of current helicity by traditional visual inspection of H$\alpha$-patterns is not reliable.

## 1. Introduction

It is widely accepted that the energy source for non-stationary processes in the solar corona is the magnetic field energy stored in the form of electric currents. Since flares seemingly can occur in any active region, the energy build up mechanism must be easy accessible for all solar active regions.

A well known conception for the generation of large-scale current systems in active regions is shearing motions in the photosphere on the scale at least of sunspot size (e.g. Hagyard *et al.*, 1984; Abramenko, Gopasyuk and Ogir, 1991). New conceptions of the magnetic energy build-up based on helical nature of solar magnetic fields were proposed recently. Rust and Kumar (1994) shown that such non-stationary processes as "filament eruptions, coronal mass ejections and active region loop expansions follow from the build-up of magnetic helicity in emerged flux ropes." Seehafer (1994) shown that the current helicity is of particular importans in the magnetic energy build-up. If we suggest that coronal fields evolve through sequences of force-free states, the energy of small-scale fluctuations of magnetic field and velocity, propagating upward from the photosphere along the field, can be transferred to the equilibrium magnetic field energy (Seehafer, 1994). This is equivalent to the generation of an electromotive force parallel to the equilibrium field (the alpha-effect). As it follows from (23) of Seehafer (1994), if the alpha-effect acts in some volume $V$, then there is a predominant (over the volume $V$) sign of the current helicity

$$H_c = \mathbf{B} \cdot (\nabla \times \mathbf{B}). \tag{1}$$

The main purpose of the present paper is to check whether there is a predominant sign of the current helicity at the photosphere of various active regions.

If a spot has a well-pronounced vortex structure, it is possible to determine the sign of current helicity, because it coincides with the sign of $\alpha$ in equation for force-free field: $\nabla \times \mathbf{B} = \alpha \mathbf{B}$ (Seehafer, 1990). Comparing the configuration of force-free field lines with a vortex-like H$\alpha$-filament configuration, one can choose an $\alpha$ (at least the sign of $\alpha$) that corresponds to the best fit. So the sign of the current helicity in a vortical magnetic structure may be determined. Seehafer (1990) studied 16 active regions and concluded that $\alpha$ is predominantly negative (positive) in the northern (southern) hemisphere. Negative (positive) current helicity corresponds to a counter-clockwise (clockwise) vortex. Thus, this result is in a good accordance with Hale's sign rule (Hale, 1927): "about 80 percent of the high level hydrogen whirls, in all sunspot cycles, are counter-clockwise in the northern hemisphere and clockwise in the southern hemisphere". This inference, confirmed later by many authors (Richardson, 1941; McIntosh, 1979; Ding, Hong and Wang, 1987) suggests that the regular vortex structure of sunspots is usually caused by the forces of rotation of the Sun (Coriolis force and/or differential rotation).

However, a considerable number of active regions have a very complex magnetic and H$\alpha$ structures, so that it becomes impossible to discover the predominant twisting by visual inspection. Nakagawa *et al.* (1971) investigated the shape of H$\alpha$ fibrils and filaments in ARs and could find no predominance of clockwise or counter-clockwise curvature of fibrils or filaments. Such an ambiguity may be caused by a projection effect or by real fragments of vortices with opposite direction in a spot. It is desirable to estimate the sign of the predominant current helicity over an AR without the necessity of comparing modeled and observed vortex structures.

It is worth while to obtain a quantitative estimate of the imbalance of current helicity over an AR area using vector magnetic field measurements in the photosphere. The value of such an imbalance could tell us if there is in the AR the possibility of large scale current build up due to the alpha-effect. And the sign of the current helicity imbalance will show the direction of the predominant twisting.

Reliable magnetic field measurements are restricted to the photospheric level, hence we can calculate only a part of the current helicity: $B_z \cdot (\nabla \times \mathbf{B})_z$ on the photosphere.

## 2. Observational Data

We analyzed vector magnetic field data obtained with the Solar Magnetic Field Telescope (SMFT) of Huairou Solar Observing Station of Beijing Astronomical Observatory (Ai, 1987). The field of view of the SMFT is about $5.23' \times 3.63'$ ($512 \times 512$ pixels of CCD). The data were averaged over $3 \times 4$ pixels. We have used the photospheric vector magnetograms recorded in the Fe I $\lambda$5324.19Å spectral line. It is a broad line with a width of about 0.33Å and Lande factor 1.5. For such a strong and broad line the Zeeman saturation and Doppler shift are not important (Ai, Li and Zhang 1982).

The magnetic field vector in the photosphere was obtained on the basis of measurements of four Stokes parameters *I, V, Q, U.* Parameter $V$ was measured in the wing of the line $\lambda$5324.19Å at the distance -0.075Å from the line center, and $Q$ and $U$ parameters were measured at the line center. The passband of the birefringent filter is 0.15Å.

Calibration of vector magnetograms is based on the following formulae:

$$B_{\parallel} = C_{\parallel} \frac{V}{I},$$

$$B_{\perp} = C_{\perp} \left( \frac{Q^2}{I^2} + \frac{U^2}{I^2} \right)^{1/4},$$

where $C_{\parallel}$ and $C_{\perp}$ are calibration coefficients for the line-of-sight and transverse magnetograms respectively (Ai, Li and Zhang 1982; Wang *et al.*, 1995). The orientation angle $\phi$ of the transverse field was determined as follows:

$$\phi = \frac{1}{2} \arctan \left( \frac{U}{Q} \right).$$

After 256-frame integration, the noise level of the measurements of the line-of-sight magnetograms is less then 20 G; for transverse magnetograms with the same integration time it is about 100 G (Wang, *et al.*, 1995).

The 180 degree ambiguity of the transverse field was resolved according the potential field approximation method (Wang, Xu, and Zhang, 1994), taking into account the evolution of an AR and the orientation of chromospheric fibrils.

We chose 40 active regions located near the central meridian and recorded with good seeing conditions. For high-latitude active regions the projection effect was removed according to the formulae of Gary and Hagyard (1990). Various of magnetic configurations are represented among these 40 ARs: unipolar spots, $\delta$-configurations, bipolar groups at different stages of evolution. They are presented in Table I.

## 3. Method

According to the definition (1) of current helicity, to calculate its value in some point one must have $\nabla\times\mathbf{B}$. If $\mathbf{B}$ is available only in the photosphere, and

$$j_z = \frac{c}{4\pi}(\nabla \times \mathbf{B})_z,$$

we can calculate a part of the current helicity $h_c$ in the photosphere:

$$h_c = B_z \cdot \frac{4\pi}{c} j_z. \tag{2}$$

The vertical electric current density was calculated on the basis the following expression:

$$j_z = \frac{c}{4\pi s} \oint_L \mathbf{B}_\perp \cdot d\mathbf{r}$$

where $\mathbf{B}_\perp$ is the vector of transverse magnetic field, $s$ is the surface enclosed by contour $L$. In our calculations the contour $L$ enclosed an area $5 \times 5$ pixels around the central point where the current density $j_z$ was determined. Integration along each side of the $L$ was performed by Simpson's formula.

Electric currents, obtained in this way and from differential formulae with subsequent smoothing (Wang, Xu, and Zhang, 1994) are in good agreement.

To test our currents calculation routine we determined the electric currents in NOAA AR 6233 and compared them with current structures obtained for the same AR by Wang *et al.* (1995) using the FFT method with subsequent smoothing. In both approaches the main current structures are quite similar but in our routine peaks are higher and structures are more jagged.

The noise level in our calculations was about 0.004 $\mathrm{A\cdot m^{-2}}$, whereas the maximal values of the current density was about 0.04-0.06 $\mathrm{A \cdot m^{-2}}$.

Our main aim was to reveal whether there is a predominant sign of current helicity $h_c$, as calculated by (2) over an active region. The most appropriate parameter for this should be the imbalance of the current helicity over an active region determined as:

$$\rho_h = \frac{\sum_{S_+} |h_c(i,j)| - \sum_{S_-} |h_c(i,j)|}{\sum_{S_+} |h_c(i,j)| + \sum_{S_-} |h_c(i,j)|} \cdot 100\%, \tag{3}$$

where $h_c(i,j)$ is the value of current helicity in a given pixel $(i,j)$, $S_+$ is a set of pixels with $h_c(i,j) > 0$ and $S_-$ is the set of pixels with $h_c(i,j) < 0$. The values $\rho_h$ are shown in the 4-th column on the Table I. Also in the 5-th and 6-th columns of the Table I the imbalance $\rho_c$ of vertical electric currents and the imbalance $\rho_B$ of vertical magnetic field component are shown. $\rho_c$ and $\rho_B$ were calculated by formulae similar to (3).

## 4. Results

It follows from Table I that in 90% of cases the imbalance $\rho_h$ of current helicity $h_c$ over an active region was quite significant: only in 4 cases out of 40 were the values $\rho_h$ close to zero. This means that in most cases there was the necessary condition for the growth of magnetic field energy due to the alpha-effect on the scale of a whole active region.

Further, in 82.5% of cases the predominant current helicity was negative ($\rho_h < 0$) in the northern hemisphere and positive ($\rho_h > 0$) in the southern hemisphere. This inference allows to suspect that Hale's sign rule is valid for different types of active regions, not only for unipolar spots with obvious vortex structure.

The distribution of imbalance of current helicity in an AR versus latitude, is shown in Figure 1. The points are located predominantly in the 2-nd and 4-th quadrants. Unipolar spots (denoted by open circles) tend to have a stronger imbalance of current helicity than other magnetic structures at the same latitude; three of the four $\delta$-configurations (denoted by star) have extremal locations on the diagram, showing high values of $\rho_h$ at high latitudes. Three $\delta$-configurations obey Hale's sign rule, but one (AR 5747) does not. In the northern hemisphere two ARs do not obey Hale's sign rule.

The possible reasons for such situations seem to clear up by inspection of maps of the vector magnetic field along with the maps of current helicity values $h_c(i,j)$ (see Figures 2-8).

Often in large bipolar sunspot groups Hale's vortices may be observed in both leading and following parts, as in the AR 6757 (Figure 2). In agreement with Hale's rule the vortices are counter-clockwise. In this AR we found negative predominant current helicity in both leading and following parts. The total imbalance of the current helicity over the entire AR was about -23%. But sometimes the structure of the magnetic field is quite complex on a small-scale, and to discover the predominant twisting from the transverse field orientation or from H$\alpha$-fibrils is rather difficult, whereas the map of $h_c(i,j)$ shows the predominance of current helicity of some sign. For example, in AR 6805 (Figure 3) only the main spot in the following part of the AR shows the well-pronounced counter-clockwise vortex. The leading spots without obvious vortices are rather weak. At the same time the map of the current helicity $h_c$ shows that in the leading part of the AR negative current helicity also dominated.

The more interesting situation was met in AR 7496 (Figure 4). It was impossible to find any predominant vortex in any spot by visual inspection of the transverse field. The map of current helicity showed the predominance of negative current helicity in the leading spot (in accordance with Hale's sign rule) and a large excess of positive helicity in the following spot (this spot grew rapidly on that day). So the imbalance $\rho_h$ of current helicity over the entire active region turned out to be positive — against Hale's rule. A similar situation, when the leading spot of an active region has an excess of current helicity in accordance with Hale's rule and the following spot has an opposite excess of current helicity, was met also in AR 6860 and in AR 6001. In such ARs the leading magnetic structure seems to be twisted by the forces of rotation of the Sun (Coriolis force and/or differential rotation), whereas in the following part most probably local subphotospheric motions create their own predominant twisting. But in any case both in the leading and in the following magnetic systems a significant imbalance of current helicity took place, thus there was the necessary condition for the growth of magnetic field energy due to the alpha-effect.

In $\delta$-configurations sometimes the regular Hale's vortex seems to be enhanced by local motions in the magnetic complex, then magnetic structures with a strong imbalance of current helicity can occur (in our study: ARs 7321, 6891, 6659; see Table I and Figure 1). One can see the well-pronounced counter-clockwise vortex of transverse magnetic field in AR 6659 in Figure 2 of Zhang and Wang (1994). But occasionally a regular vortex seems to be significantly distorted by local processes, and large patterns of opposite rotation appear, as in the AR 5747 (Figure 5) and in the AR 5612 (Figure 6). The imbalance of current helicity may be close to zero (AR 5612) or even of opposite sign (AR 5747).

All unipolar symmetric spots in our analysis obeyed Hale's sign rule, thus one can suggest that local motions either are negligible or act in the same direction as the regular forces of differential rotation in twisting of such a magnetic structure. This kind of magnetic configurations showed in our analysis the highest value of current helicity imbalance — up to 74.6% in AR 7294 (Figure 7).

We have met with one active region (AR 6064, Figure 8) which was large and bipolar, and its main spots showed no vortices so its transverse field structure was potential-like. Calculation of (total over the AR) imbalance of current helicity gave the value about zero. Apparently, in such a bipolar quasi-potential active region there were no conditions for the growth of magnetic field energy due to the alpha-effect on the scale of the whole active region.

## 5. Conclusions

The way (dc) magnetic field energy builds up in the corona above an active region is not completely clear. Seehafer (1994), under the assumption that the magnetic field evolves through the sequence of force-free states, theoretically shown that the energy of small-scale fluctuations of magnetic and velocity fields can be transferred into the energy of large-scale currents in an AR. The necessary condition may be indicated by the presence of a predominant sign of current helicity over some volume, in particular, over the whole active region. Here we attempted to find how frequently such a condition may take place on the scale of whole ARs.

Using the data of measurements of the magnetic field vector in the photosphere we calculated the current helicity (more precisely, the part of helicity: $B_z \cdot (\nabla \times \mathbf{B})_z$)

over the whole AR area for 40 active regions of 22 solar activity cycle. Among them here were sunspot groups of various kinds: unipolar spots, $\delta$-configurations, bipolar active regions at different stages of evolution.

Analyzing the distribution of current helicity over the area of every active region we have come to the following conclusions:

1) In 90% of cases, there existed significant excess current helicity of some sign over the active region area. This means that in 90% of cases the necessary condition for the growth of magnetic field energy due to the alpha-effect on the scale on the whole active region was met. This result permits to suggest that the build up of large-scale currents in an active region due to small-scale fluctuations may be a rather typical phenomenon in ARs, if the magnetic field evolves through the sequence of force-free states.

2) The negative (positive) excess of current helicity over some area means that magnetic structure in the area has a predominant counter-clockwise (clockwise) twisting. So, Hale's sign rule (the predominance of counter-clockwise (clockwise) vortices in the northern (southern) hemisphere) was satisfied in 82.5% of cases in our analysis. Such an asymmetry allows to suggest that Hale's sign rule is valid not only for unipolar spots with obvious vortex structure (Hale, 1927; Richardson, 1941; McIntosh, 1979; Ding, Hong and Wang, 1987; Seehafer, 1990;), but also for ARs of different types. The forces of rotation of the Sun (Coriolis force and/or differential rotation) seem to take effect in twisting of various magnetic structures.

3) Regular forces of rotation of the Sun seems to be superposed by local processes in formation of a resulting vortex around a spot.

4) The imbalance of current helicity does depend on the imbalance of magnetic flux and the imbalance of vertical currents. The imbalance $\rho_B$ of magnetic flux varies in large limits (from -41% to 58%, see Table I), whereas the imbalance $\rho_c$ of vertical currents is rather small value: less then 3.5%.

Results obtained here are in good agreement with qualitative inferences based on the traditional method of visual inspection of the field lines curvature.

Our method allows to study both the imbalance and the distribution of current helicity over the AR's area. The method can be applied to those ARs where the determination of the predominant sign of current helicity by traditional visual inspection of H$\alpha$-patterns is not reliable.

## Acknowledgments

This research was supported by the Chinese Academy of Sciences and by the Ukrainian Government Committee of Science and Technology. The authors (VIA and VBY) are most grateful to Professor Guoxiang Ai for kind hospitality at Beijing Astronomical Observatory. VIA would like to thank Professor Jingxiu Wang for helpful discussion. We are indebted to the staff of Huairou Solar Observing Station for their assistance in obtaining the data. VBY is delighted to acknowledge the International Renaissance Foundation for his financial support.

We would like to acknowledge the careful reading and useful comments made by the referee.

## References


Abramenko, V.I., Gopasyuk, S.I., and Ogir, M.B.: 1991, *Solar Phys.* **134**, 287.

Ai, G., Li, W., and Zhang, H.: 1982, *Chin. Astron. Astrophys.* **6**, 129.

Ai, G.: 1987, *Publ. Beijing Astron. Obs.* **9**, 27.

Ding, Y.J., Hong, Q.F., and Wang, H.Z.: 1987, *Solar Phys.* **107**, 221.

Gary, G.A., and Hagyard, M.J.: 1990, *Solar Phys.* **126**, 21.

Hagyard, M.J., Smith, J.B., Teuber, D., West, E.A.: 1984, *Solar Phys.* **91**, 115.

Hale, G.E.:1927, *Nature*, **119**, 708.

McIntosh, P.S.: 1979, *Upper Atmosphere Geophysics Report UAG-70*, World Data Center A for Solar-Terrestrial Physics, Boulder

Nakagawa, Y., Raadu, M.A., Billings, D.E., McNamara, D.: 1971, *Solar Phys.* **19**, 72.

Richardson, R.S.: 1941, *Astrophys. J.* **93**, 24.

Rust, D.M. and Kumar, A.: 1994, in *Proc. of the Third SOHO Workshop – Solar Dynamic Phenomena and Solar Wind Consequences*, European Space Agency SP-373, p.39.

Seehafer, N.: 1990, *Solar Phys.* **125**, 219.

Seehafer, N.: 1994, *Astron. Astrophys.* **284**, 593.

Wang, J., Shi, Z., Wang, H., and Lu, Y.: 1995, *Astrophys. J.* (in press).

Wang, T., Xu, A., and Zhang, H.: 1994, *Solar Phys.* **155**, 99.

Zhang, H., and Wang, T.: 1994, *Solar Phys.* **151**, 129.

Table 1. Imbalances $\rho_h, \rho_c, \rho_B$ (over an active region) of current helicity, electric current and magnetic field flux, respectively.

| NOAA AR | Date | Coordinate | $\rho_h$,% | $\rho_c$,% | $\rho_B$,% |
|---|---|---|---|---|---|
| northern hemisphere | | | | | |
| 5617 | 31 Jul 1989 | N19 W15 | -4.50 | 1.5 | 30.0 |
| 5680 | 11 Sep 1989 | N15 E04 | -27.1 | 1.0 | -16.5 |
| 5738 | 13 Oct 1989 | N11 E10 | -11.1 | 1.7 | 1.2 |
| 5782 | 8 Nov 1989 | N15 E24 | -34.7 | 2.2 | 5.8 |
| 5948 | 26 Feb 1990 | N16 E02 | -27.8 | 1.4 | -13.5 |
| 6001 | 6 Apr 1990 | N16 E04 | 14.0 | 0.5 | 2.8 |
| 6233 | 30 Aug 1990 | N12 W15 | -46.5 | 1.2 | -18.8 |
| 6659* | 9 Jun 1991 | N29 W05 | -25.4 | 0.6 | -41.5 |
| 6757 | 4 Aug 1991 | N18 W09 | -26.1 | 1.2 | 18.0 |
| 6805 | 31 Aug 1991 | N20 E00 | 22.6 | 0.8 | 39.3 |
| 6855 | 3 Oct 1991 | N14 E10 | -26.6 | -0.4 | 3.1 |
| 7205 | 19 Jun 1992 | N12 E10 | -37.6 | 0.3 | 8.5 |
| 7216 | 4 Jul 1992 | N12 E12 | -9.5 | 1.4 | 7.1 |
| 7315 | 22 Oct 1992 | N05 W08 | -15.8 | 0.7 | -4.9 |
| 7496 | 9 May 1993 | N14 E08 | 19.2 | 0.4 | -15.8 |
| 7532 | 25 Jun 1993 | N06 W14 | -18.3 | 0.2 | -34.9 |
| 7590 | 3 Oct 1993 | N13 E05 | -5.8 | 0.2 | -3.3 |
| 7722° | 18 May 1994 | N08 W02 | -14.1 | 0.8 | -38.9 |
| 7779 | 18 Sep 1994 | N17 E10 | -17.2 | -0.7 | 0.6 |
| southern hemisphere | | | | | |
| 5047° | 20 Jun 1988 | S15 E11 | 25.4 | 0.8 | 23.4 |
| 5612 | 3 Aug 1989 | S16 W04 | 0.4 | 1.4 | 26.9 |
| 5634 | 12 Aug 1989 | S14 W04 | 9.3 | 1.9 | 8.4 |
| 5747* | 20 Oct 1989 | S26 W01 | -45.7 | 0.2 | 21.5 |
| 6064 | 20 May 1990 | S14 W14 | 0.8 | 0.8 | 3.6 |
| 6279° | 21 Sep 1990 | S09 W02 | 32.5 | 3.5 | 9.6 |
| 6786 | 21 Aug 1991 | S10 W06 | 16.6 | 2.6 | 18.6 |
| 6853 | 3 Oct 1991 | S16 W20 | -0.5 | 0.3 | 6.0 |
| 6880 | 3 Oct 1991 | S23 W09 | -0.2 | 0.2 | -2.1 |
| 6891* | 29 Oct 1991 | S14 W05 | 33.1 | 0.2 | 31.6 |
| 7289° | 26 Sep 1992 | S12 E00 | 48.9 | 0.3 | 17.4 |
| 7294° | 29 Sep 1992 | S12 E18 | 74.6 | 0.7 | 58.2 |
| 7316 | 23 Oct 1992 | S10 E12 | 23.8 | 0.2 | 18.3 |
| 7321* | 26 Oct 1992 | S23 W04 | 44.2 | -0.2 | 7.8 |
| 7518 | 6 Jun 1993 | S11 W06 | 14.5 | 1.1 | 8.8 |
| 7529° | 29 Jun 1993 | S10 W04 | 64.7 | 0.6 | 21.1 |
| 7585 | 25 Sep 1993 | S10 E01 | 18.8 | -0.6 | 5.2 |
| 7597 | 15 Oct 1993 | S16 W03 | 12.5 | 0.5 | -21.5 |
| 7764 | 17 Aug 1994 | S05 E01 | 35.3 | 0.9 | 3.0 |
| 7773 | 6 Sep 1994 | S06 W08 | 16.8 | -0.6 | -3.1 |
| 7776° | 18 Sep 1994 | S05 W16 | 33.3 | -0.9 | 6.6 |

$*\delta$-configuration  $\circ$ unipolar spot

**Fig. 1.** Distribution of the imbalance $\rho_h$ of current helicity $h_c$ in % (horisontal axis)in an AR versus the latitude of an AR (vertical axis).

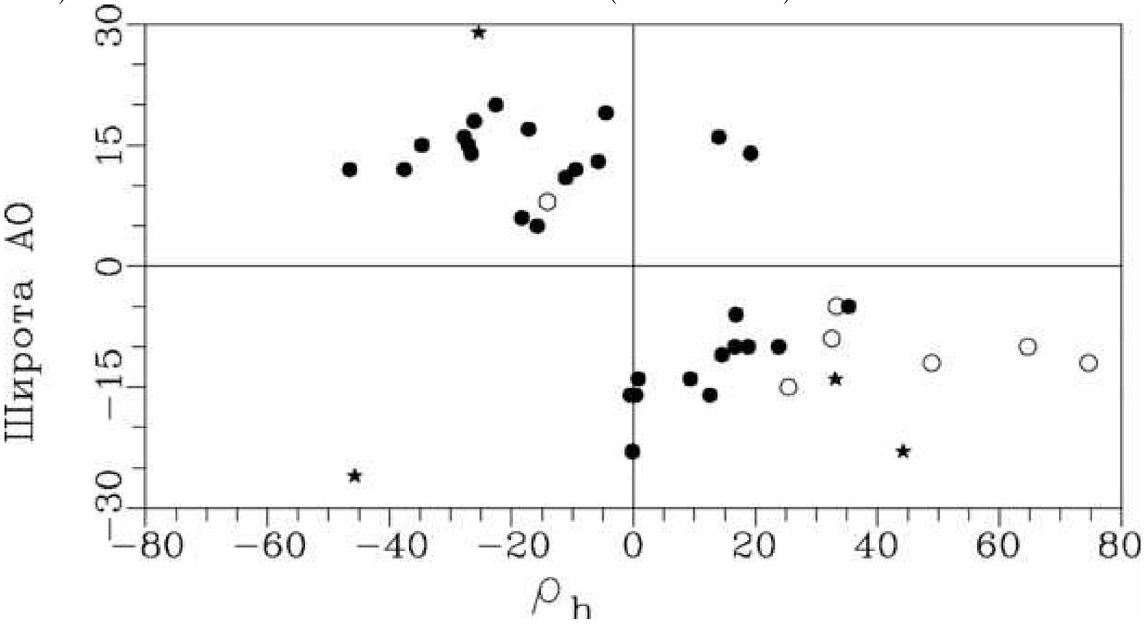

**Fig. 2.** The map of magnetic field vector (contour levels of longitudinal component refer to 200, 500, 1000, 1500, 2000, 2500 G, top panel) and the map of the current helicity (contour levels refer to 1, 5, 10, 20, 40, A · m $^{-2}$, bottom panel) on the AR 6757.

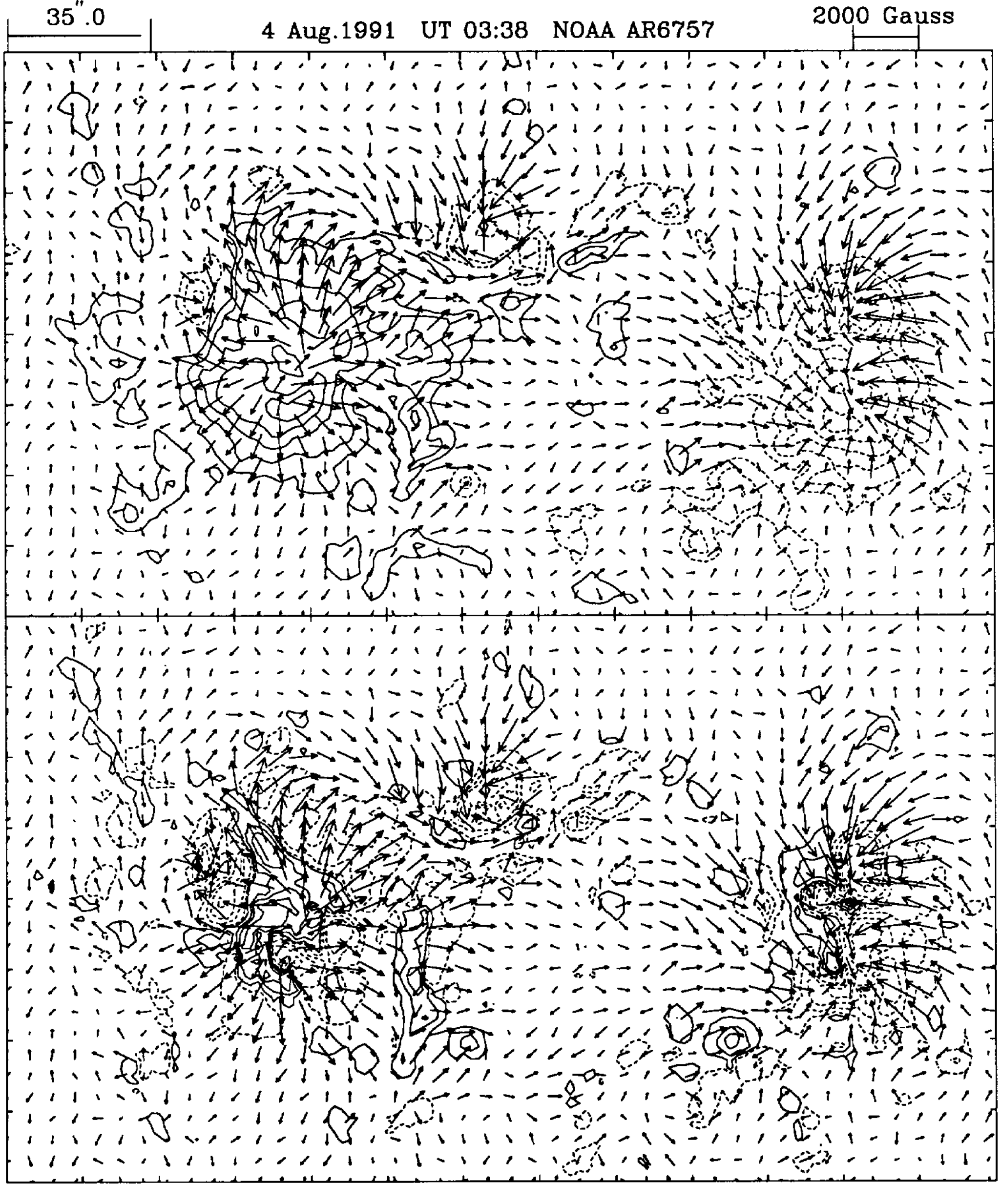

**Fig. 3.** The map of magnetic field vector and the map of the current helicity on the AR 6805. Notations are the same as in Figure 2.

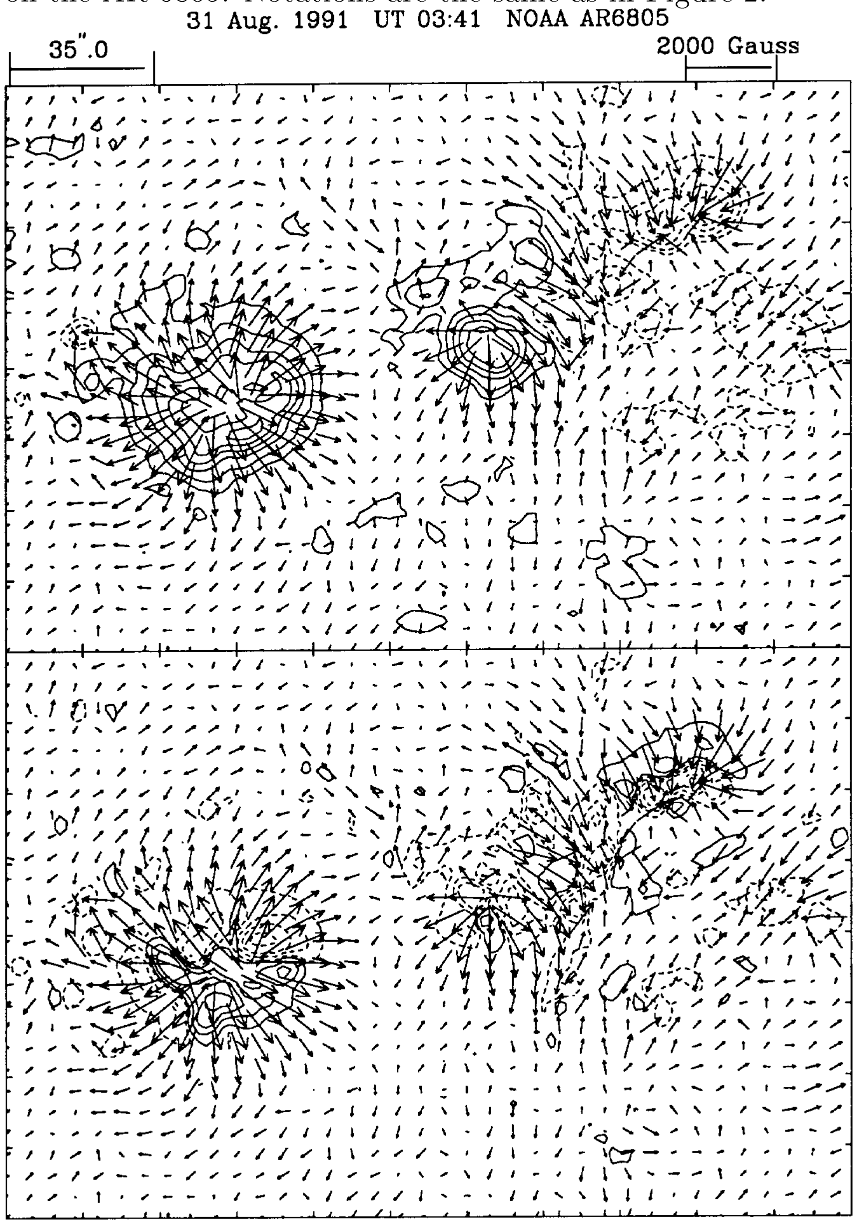

**Fig. 4.** The map of magnetic field vector and the map of the current helicity on the AR 7496. Notations are the same as in Figure 2.

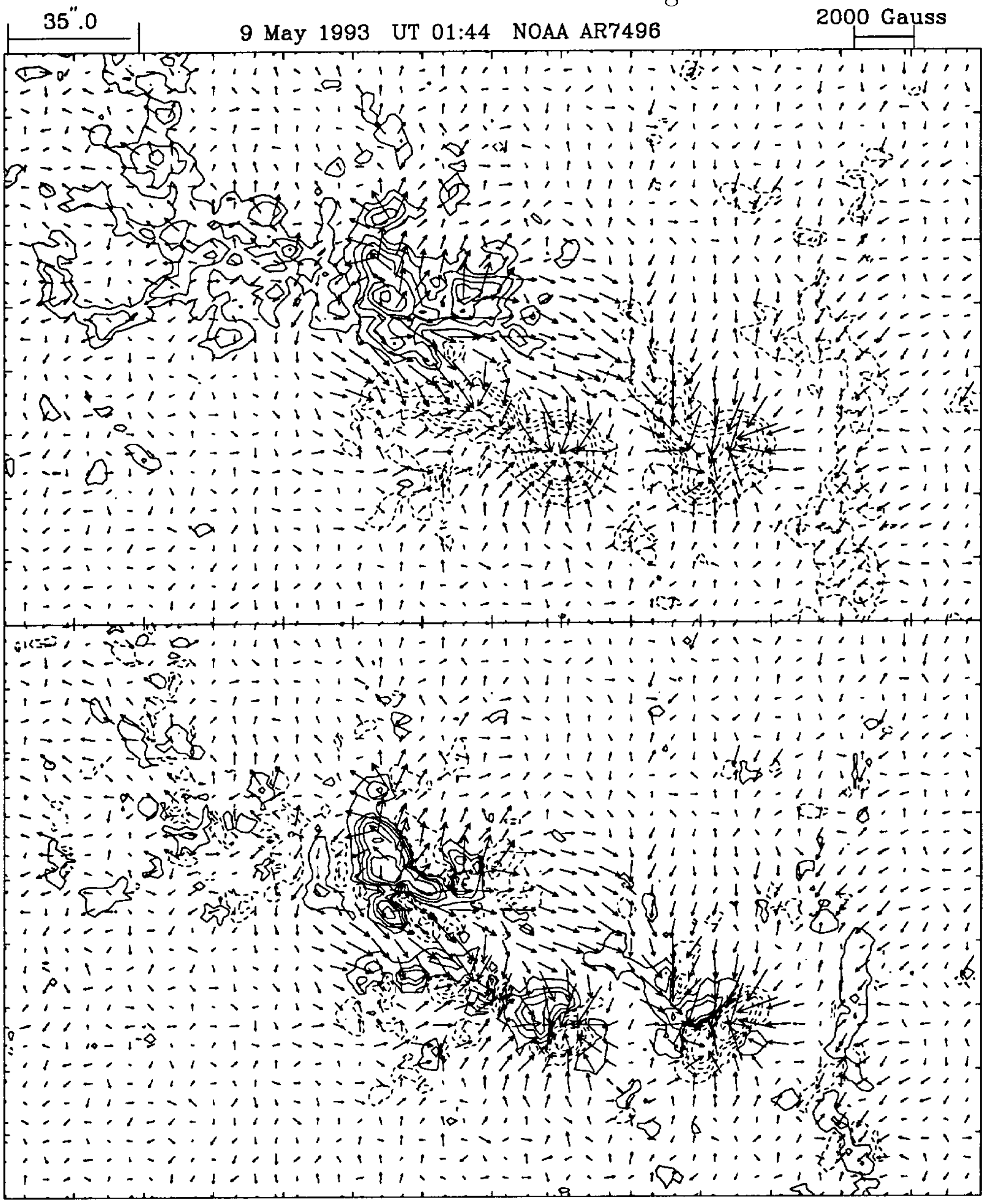

**Fig. 5.** The map of magnetic field vector and the map of the current helicity on the AR 5747. Notations are the same as in Figure 2.

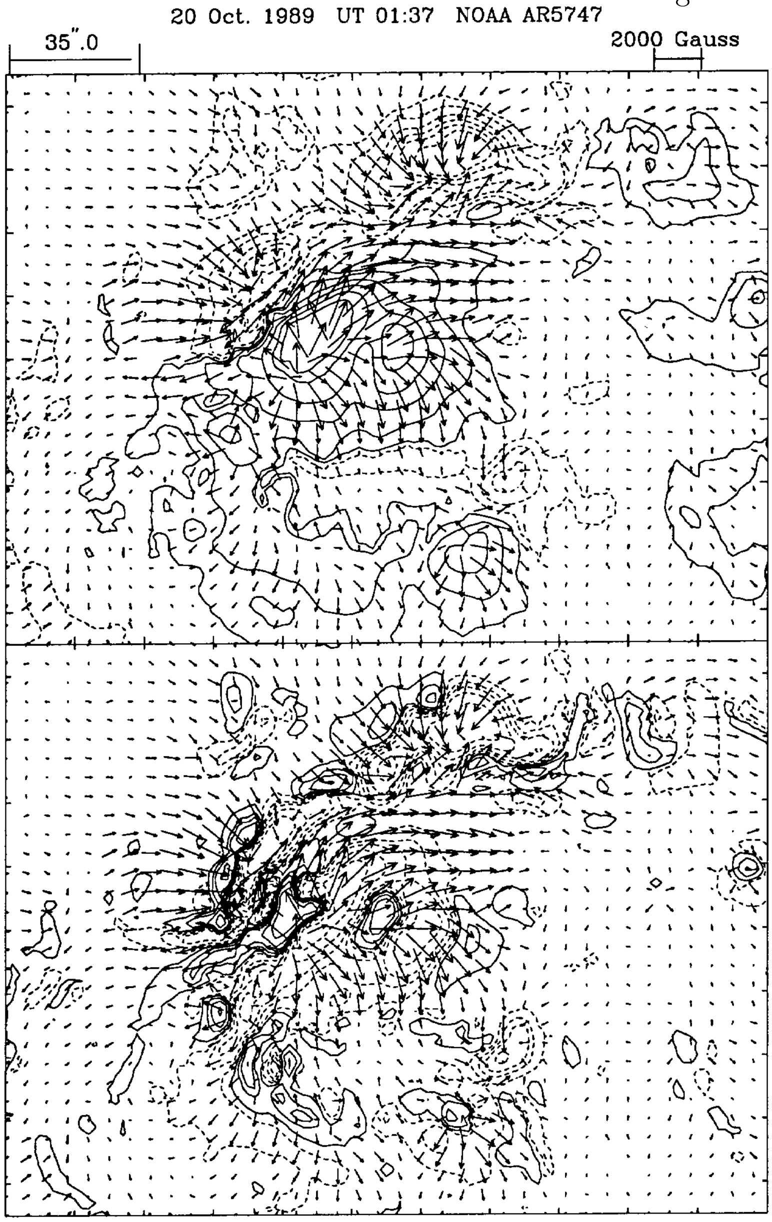

**Fig. 6.** The map of magnetic field vector and the map of the current helicity on the AR 5612. Notations are the same as in Figure 2.

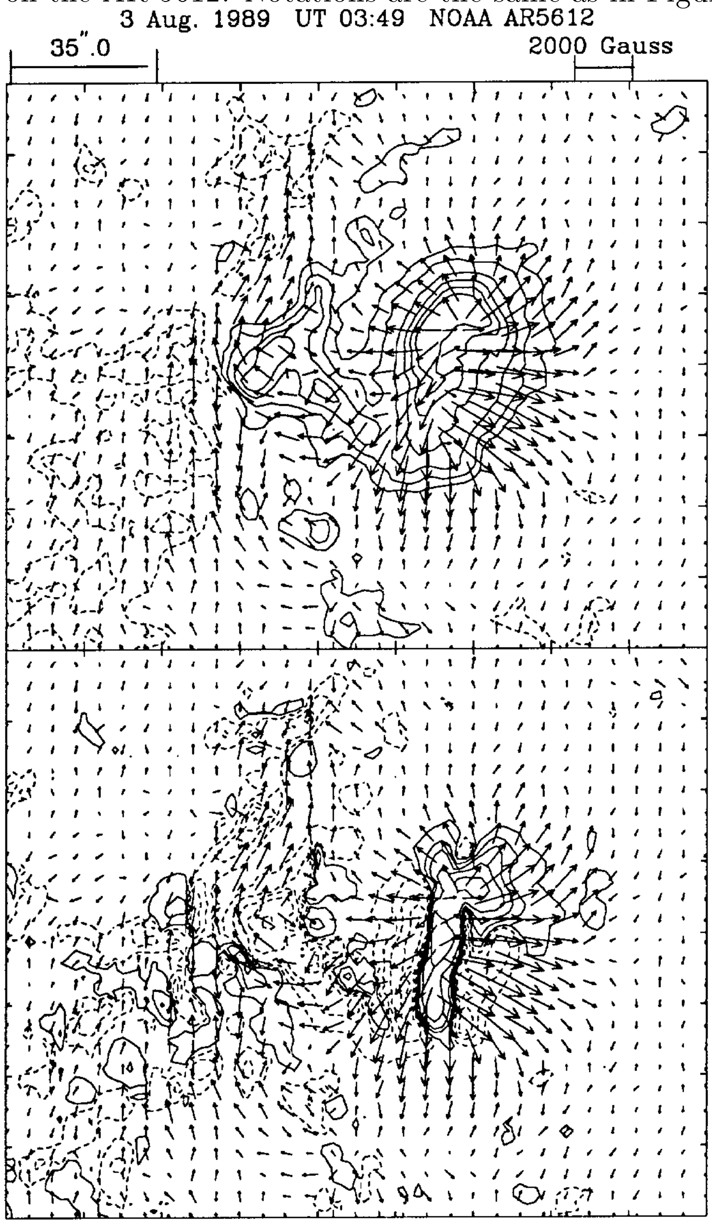

**Fig. 7.** The map of magnetic field vector and the map of the current helicity on the AR 7294. Notations are the same as in Figure 2.

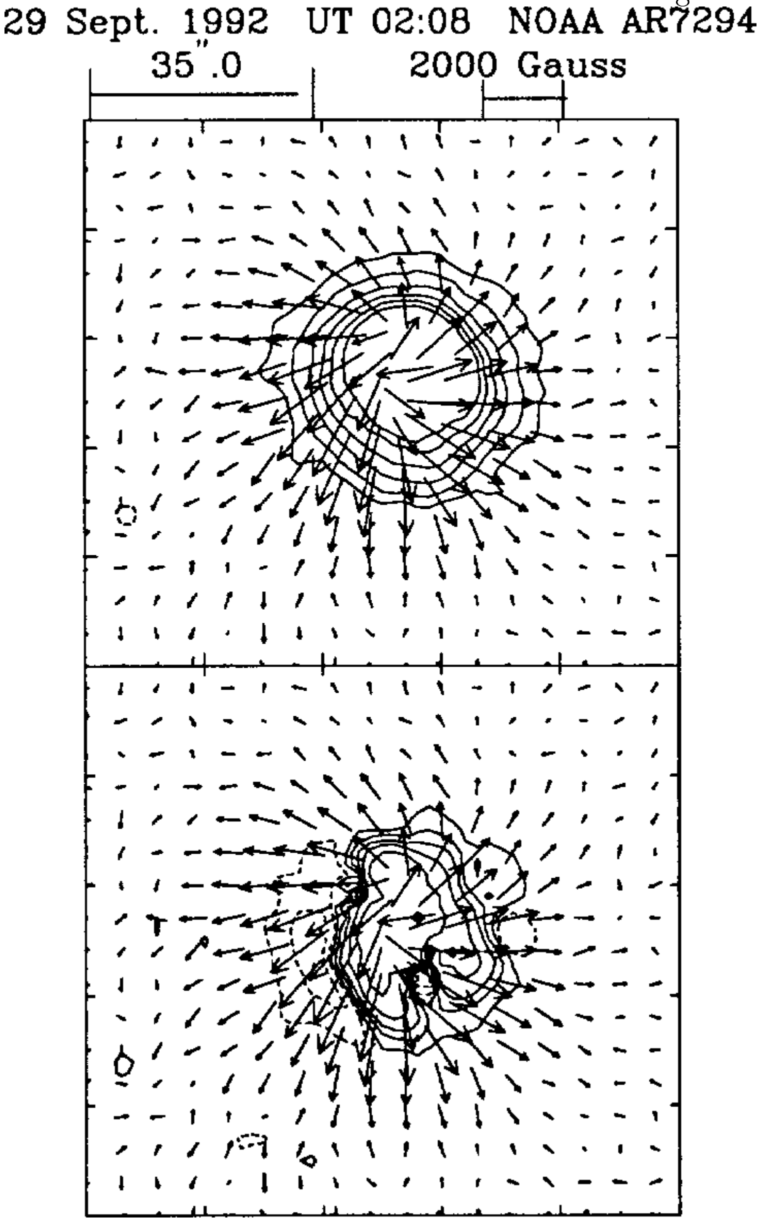

**Fig. 8.** The map of magnetic field vector and the map of the current helicity on the AR 6064. Notations are the same as in Figure 2.